

Characterization of Calibrated Gelatin Sponge Particles in a Rabbit Renal Embolization Model

Yongsheng Ye¹ · Yimin Ren¹ · Hanqiang Zeng² · Jianxun He¹ · Zhiwei Zhong¹ · Xiaomei Wu¹ 

Received: 4 January 2019 / Accepted: 15 April 2019 / Published online: 1 May 2019

© Springer Science+Business Media, LLC, part of Springer Nature and the Cardiovascular and Interventional Radiological Society of Europe (CIRSE) 2019

Abstract

Purpose To evaluate the level of artery occlusion, degradation periods, tissue response and vessel recanalization of calibrated gelatin sponge particles after segmental renal artery embolization.

Materials and Methods Superselective embolization of 14 adult rabbits was performed with calibrated gelatin sponge particles (150–350 μm). Two rabbits were killed immediately after the procedure (day 0). One pair of rabbits was killed on each of the following days: 1, 3, 7, 14, 28 and 56. One rabbit from each pair underwent CT angiography before embolization and killing. The pathologic changes of the embolized renal parenchyma and embolic characteristics of calibrated gelatin sponge particles were evaluated histologically and angiographically.

Results Calibrated gelatin sponge particles were distally located in interlobular artery with a dense packing on day 0. The level of occlusion paralleled the size of the particles. Partial degradation of the particles was observed on day 3, and complete degradation was observed on day 14. Vessel recanalization was observed through both CTA and histological analysis starting on day 3. Vascular inflammation responding to gelatin sponge particles was mild and subsided with the degradation of the particles. On day 28 and day 56, attenuation of embolized vessels occurred due to

marked intimal proliferation, and vascular occlusion developed.

Conclusions Gelatin sponge particles of 150–350 μm produced dense and distal embolization, and were resorbed before day 14 with a mild tissue reaction. Vessel recanalization occurred secondary to the resorption of gelatin sponge particles, but permanent vascular occlusion developed due to marked intimal hyperplasia after day 28.

Keywords Embolization · Gelatin sponge particles · Renal artery · Animal model

Introduction

Gelatin sponge (GS) is a kind of porous and water-insoluble animal protein-based sponge with compressible and hydroexpansive properties [1]. GS produces vascular occlusion through mechanical filling of the lumen and promoting blood clotting [2]. Its particles are most widely used as a kind of bioresorbable embolic agents in the field of embolotherapy, particularly in the management of hepatocellular carcinoma [3, 4], uterine fibroids [5, 6], and massive arterial bleeding [7, 8]. GS particles have certain advantages over other embolic agents: they have been used as safe and effective embolic agents for more than 30 years in clinical practice [9], their resorbability makes them more favorable than nonresorbable materials that persist in vivo with unknown consequences [10], and they are relatively inexpensive.

However, GS particles require manual cutting, which results in size discrepancy [11], making it impossible to

✉ Xiaomei Wu
helenwinson@163.com

¹ Department of Radiology, The First Affiliated Hospital of Guangzhou Medical University, 151 Yanjiangxi Road, Guangzhou 510120, People's Republic of China

² Department of Interventional Therapy, Dongguan People's Hospital, Dongguan 523059, People's Republic of China

intentionally select the occlusion level of the vessels. Furthermore, although they are believed to degrade in the vessels within a few weeks [2], the degradation periods of these sponges cannot be strictly controlled. The development of calibrated GS (CGS) particles can largely address these shortcomings. CGS particles are obtained by sieving GS particles with standard sieves [12], and are available in a range of sizes, including 150–350, 350–560, 560–710, 710–1000, 1000–1400, and 1400–2000 μm , so that the best size can be chosen depending on the artery being embolized. Currently, CGS particles have been used in some clinical practices and have proven to be safe and effective [4, 12], but the embolic characteristics of CGS particles are still unknown. The aim of the present study was to observe the level of arterial embolization, embolic tissue response, degradation period of the embolic agent, as well as vessel recanalization on a CGS particle-induced rabbit renal segmental embolized model.

Materials and Methods

Animals and Experiment Design

The study was approved by our institutional animal care and use committee. Fourteen adult New Zealand rabbits weighing 2.0–2.5 kg were included in this study. The rabbits were divided into 7 groups according to the time of euthanasia (immediately after embolization at day 0, and day 1, 3, 7, 14, 28, 56). Each group comprised of two rabbits. All rabbits received segmental renal arterial embolization and were euthanized at specified killing time points for histological study. One rabbit from each group

(except for day 0) underwent CT angiography prior to both embolization and killing (Fig. 1).

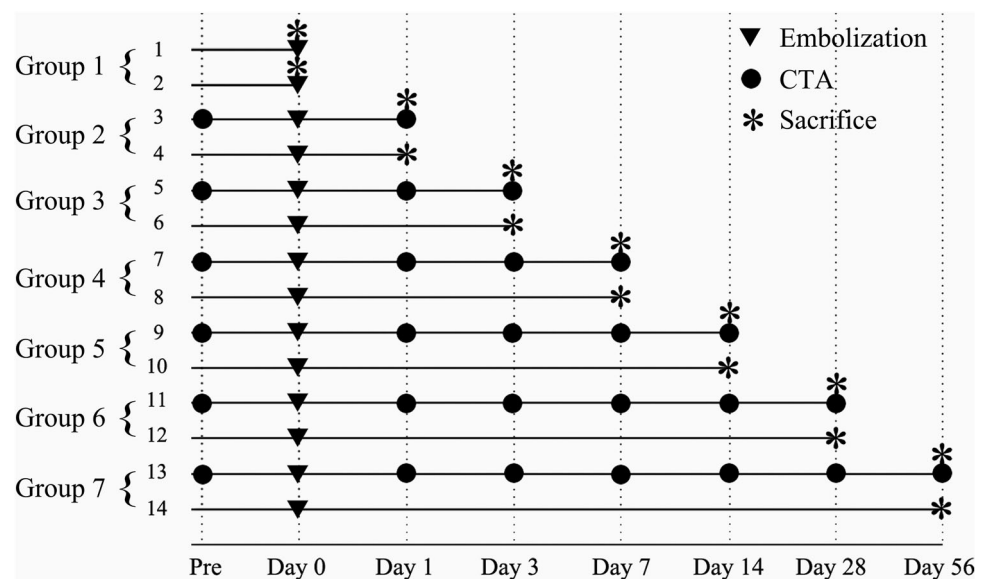
Calibrated Gelatin Sponge (CGS) Particles

CGS particles of 150–350 μm in diameter (Alikon Co., Ltd., Hangzhou, China, 100 mg/bottle) were used. The particle size distribution was assessed with an optical microscope (Nikon, Melville, New York) by measuring the smaller lengths of 200 randomly picked particles. The particles suspension with a concentration of 5 mg/mL, which was composed of 100 mg of CGS particles (one bottle) and 20 ml of 50% Iodixanol (mixed with 10 ml of saline and 10 ml of Iodixanol 320 mg/ml, GE), was used for renal embolization.

Embolization of the Renal Artery and CT Angiography (CTA)

Embolization of unilateral renal lower pole was performed from a right common carotid artery approach. The left kidney was chosen in most rabbits. The right kidney was chosen as an alternative when a left kidney was not selected easily. The rabbits were anesthetized by intramuscularly injection of 0.1 ml/kg Sumianxin II (Institute of Military Veterinary Medical Sciences, China) and 1 ml/kg 3% sodium pentobarbital (Sigma, American). A 4-F sheath was placed in the right common carotid artery after surgical exposure. Under fluoroscopic guidance, a 4-F Cobra catheter (Cordis, Johnson, American) was inserted into the renal artery and superselective catheterization of a renal branch artery supplying the lower pole was performed using a 2.7-F coaxial microcatheter (Progreat, Terumo). CGS particles were delivered into the lower pole of the

Fig. 1 The experiment process



kidney through the microcatheter at a rate of 1 mL/min until achieving stasis. The volume of particles delivered was recorded. Angiography was performed before embolization, immediately after embolization, and 10 min after embolization. The arterial access site was closed by ligation. Potential complications including rupture of blood vessel during operation, ectopic embolism, postoperative infection and accidental death were recorded.

CTA was performed using adaptive 4D spiral mode on a 128-slice CT scanner (Somatom Definition AS+; Siemens Healthcare, Germany). The parameters were as follows: tube potential, 80 kV; current, 100 mAs; collimation, 64×0.6 mm; slice thickness/gap, 1.5 mm/0.75 mm; scan range, 8 cm; scan time, 30 s. Iodinated contrast media (370 mgI/ml, Bayer, Germany) (2 mL/kg) was injected via the ear vein (flow rate 1.5 ml/s) using a CT power injector and a standard delay of 4 s. Image post-processing was implemented on a dedicated workstation (MMWP, Siemens Healthcare, Germany). Vessel recanalization in CTA was evaluated by the reperfusion of the interlobar arteries. The changes of the embolized renal parenchyma were evaluated as well.

Histopathology

The rabbits were euthanized by intravenous injection of pentobarbital. The kidneys were surgically removed and fixed in 4% formaldehyde solution. Four 5-mm-thick slices were sectioned from the lower pole of each kidney and embedded in paraffin blocks. Two 5- μ m-thick sections from each paraffin block were stained with hematoxylin and eosin. The presence of GS particles, arterial location of GS particles, coagulative necrosis, vascular inflammation, intimal hyperplasia and vessel recanalization in each stained section were evaluated by microscopy.

Descriptions of the presence of particles in arteries used the qualitative categories of most (70–100%), many (40–70%), a few (5–40%), rare (1–5%), and single fragment (< 1%), where the average number of GS particles per kidney identified at day 0 was considered as 100% [13]. The arterial locations of particles were categorized as interlobar, arcuate and interlobular. The arcuate artery coursed along the outer side of the renal medulla. The interlobular artery coursed outer than the arcuate artery. The interlobar artery coursed inner than the arcuate artery [14]. The diameter of the smallest embolized interlobular artery was measured (average of the sum of cross-sectional length and width).

Changes in renal parenchyma in ischemic areas were analyzed. Coagulative necrosis was defined as areas of renal parenchyma demonstrating loss of nuclear and cell detail with retention of architecture. Vascular inflammation associated with GS particles was semi-quantitatively

graded as follows: (a) mild: a small amount of focal or multifocal intravascular or perivascular infiltrate of inflammatory cell without evidence of vascular necrosis; (b) moderate: a modest number of intravascular or perivascular infiltrate of inflammatory cells with or without limited evidence of vascular necrosis; (c) severe: a large number of intravascular or perivascular infiltrate of inflammatory cells with some vascular necrosis [13]. Intimal hyperplasia, a nonspecific indicator for vessel injury, was defined as thickening of the intimal layer and was generally graded as absent, mild, moderate, and was marked depending on the luminal area lost. Vessel recanalization was graded according to the degree to which the original vessel luminal diameter was restored as absent, mild (up to 33% of the original lumen was restored), moderate (restoration of 34–66% of the original luminal), or marked (restoration of 67–100% of the original vessel luminal diameter) [13].

Results

Characteristics of Calibrated Gelatin Sponge Particles

The CGS particles showed as white powder by macroscopy. Under microscopy, CGS particles displayed an irregular shape and a porous structure (Fig. 2). The size distribution of the 150–350 μ m GS particles is shown in Fig. 3. 86% of the particles matched the size range of 150–350 μ m. The average size of the particles was $244 \mu\text{m} \pm 74$ (range 107–480 μ m).

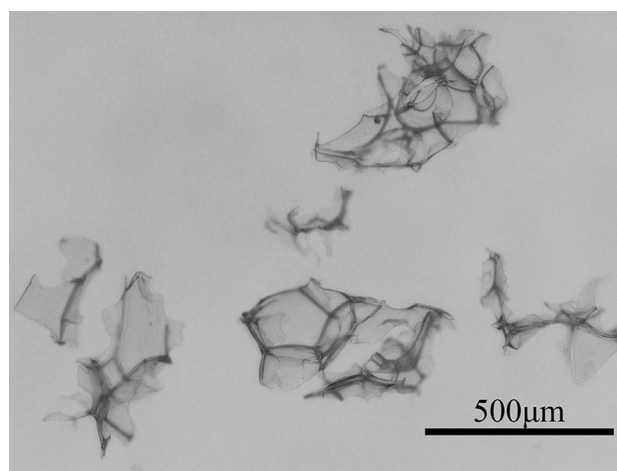


Fig. 2 Microscopic image of 150–350 μ m gelatin sponge particles

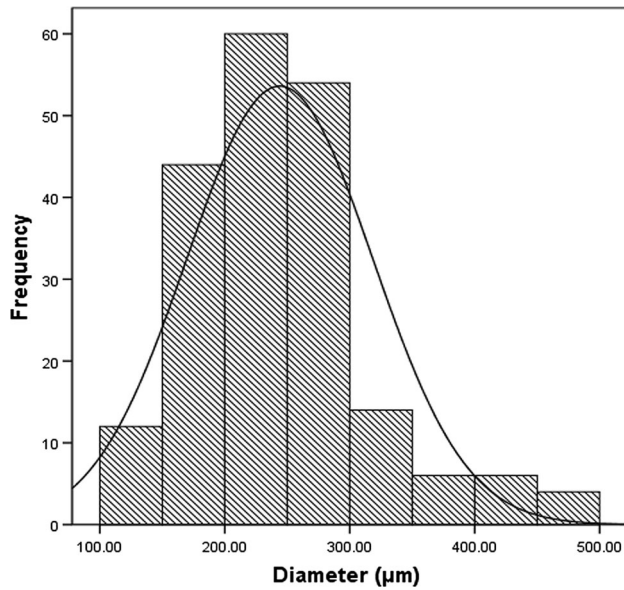


Fig. 3 Size distribution of 150–350 µm gelatin sponge particles

Segmental Embolization Procedure and CTA Findings

Segmental embolization of renal artery using CGS particles was successfully performed in all rabbits, including 12 left kidneys and 2 right kidneys. The mean volume of the particles used was $1.4 \text{ ml} \pm 0.20$. Follow-up angiography showed complete occlusion of the target vessels as a result of flow stagnation, lumen occlusion, and poor enhancement of the parenchyma (Fig. 4). No pseudoaneurysms, dissections or arterial ruptures occurred during or after embolization (after control angiogram). All rabbits survived killing without complications such as ectopic embolism, postoperative infection, and accidental death.

The target interlobar branches were not visible in CT angiography images on day 1. Reperfusion was observed on day 3, 7 and 14. Minimal calcification was observed in

parenchymal infarction on day 14, while pronounced calcification was observed after day 28. The target branches could not be distinguished due to severe calcification in parenchymal infarction on day 28 and 56. The embolized renal parenchyma was poorly enhanced at every time point (Fig. 5).

Histopathological Findings

The kidneys removed immediately after embolization (day 0) showed no evidence of infarction but exhibited reddish brown mottling on the surface. The kidneys removed at other time points displayed white-grayish discoloration on the surface of the lower pole, which implies acute regional infarction. The embolized kidneys decreased in size on day 28 and day 56, along with exhibiting renal parenchyma calcification. The histopathological findings are summarized in Table 1. The CGS particles had a blue violet color and a floccular shape. On day 0, CGS particles were clustered in interlobar, arcuate and interlobular arteries with a compact distribution. The smallest embolized interlobular artery was 124 µm in diameter. On day 1, CGS particles were still located in interlobar, arcuate and interlobular arteries with more compact distribution due to mild expansion and distortion of the particles. The smallest embolized interlobular artery was 109 µm in diameter. On day 3, many (40–70%) particles were found in interlobar and arcuate arteries. Degradation of particles was first identified on day 3 with moderate irregular distortion and decrease in size. On day 7, the particles had clearly reduced in size, and few particles fragments (< 5%) were observed in interlobar arteries. On day 14, 28 and 56, particle fragments vanished in all three arterial levels. Mild vascular recanalization was observed on day 3, and marked on day 7 and 14. No organized thrombus was observed in all observation phase. The embolized renal parenchyma showed ischemia and degeneration on day 0 and day 1,

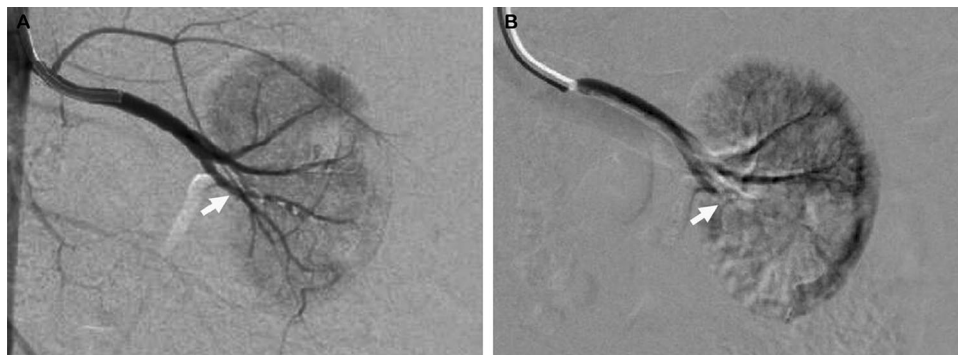


Fig. 4 Example of segmental embolization of renal arteries with calibrated gelatin sponge particles. **A** Angiogram obtained before embolization. Left renal arteries of lower pole (arrow) are opacified. **B** Angiogram obtained 10 min after embolization. The arterial branch

into the left lower pole of the kidney (arrow) was embolized, with findings of flow stagnation, lumen occlusion, and poorly enhanced areas

Fig. 5 Example of sagittal CTA images of the left kidney at different time points. **A** Before embolization, the branches of the renal arteries were observed clearly and the enhancement of the renal parenchyma was normal. **B** Day 1, the arterial branches into the lower pole of the left kidney were occluded, and the parenchyma supplied by the embolized arteries showed lack of enhancement. **C–E** Day 3, 7 and 14, the embolized arterial branches showed reperfusion. The parenchyma supplied by the embolized arteries demonstrated small amount of calcification on day 14 (arrowheads). **F** Day 28, the target branches could not be distinguished due to the pronounced calcification in parenchymal infarction (arrowheads)

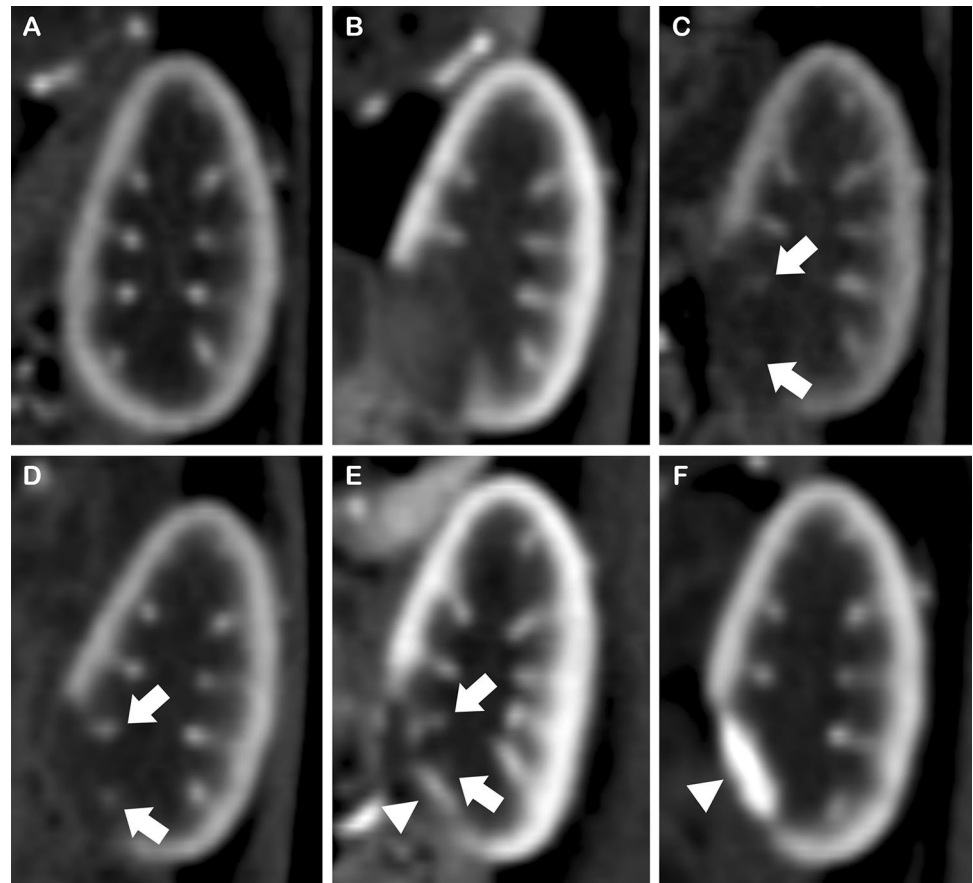


Table 1 Summary of microscopic histological findings in rabbit kidneys after embolization with CGS particles

Pathologic finding	Day 0	Day 1	Day 3	Day 7	Day 14	Day 28	Day 56
Particles present	Most	Most	Many	A few	Absent	Absent	Absent
Particles location	Interlobar	Interlobar	Interlobar	Interlobar	Absent	Absent	Absent
	Arcuate	Arcuate	Arcuate				
	Interlobular	Interlobular					
Coagulative necrosis	Absent	Mild	Marked	Marked	Marked	Fibrosis Mineralization	Fibrosis Mineralization
Vascular inflammation	Absent	Mild	Mild	Mild	Mild	Absent	Absent
Intimal proliferation	Absent	Absent	Absent	Absent	Absent	Marked	Marked
Recanalization	Absent	Absent	Mild	Marked	Marked	Absent	Absent

infarction on day 3 to day 14, and fibrosis and mineralization on day 28 and day 56, respectively. Mild vascular inflammation was identified on day 1 to day 14. Few inflammatory cells were found in the intravascular and perivascular areas on day 1. The inflammatory cells increased significantly on day 3, followed by a decrease on day 7 and day 14. The vascular inflammation resolved as particles fully degraded on day 28 and 56. Marked intimal hyperplasia was identified both on day 28 and day 56, resulting in stenosis and reocclusion of the recanalization vessels (Fig. 6).

Discussion

Hand-cut GS particles have the risk of producing an overly proximal embolization, which is generated by large particles, or producing an overly distal embolization, which is generated by small particles [15]. Katsumori and Kasahara [11] showed that cutting GS sheets with scissors into cubes of approximately 1–1.5 mm × 1–1.5 mm would give particles with a wide size distribution ranging 500 and 2000 μm. Our study demonstrated that the level of occlusion depends on the size of CGS particles. The precise size

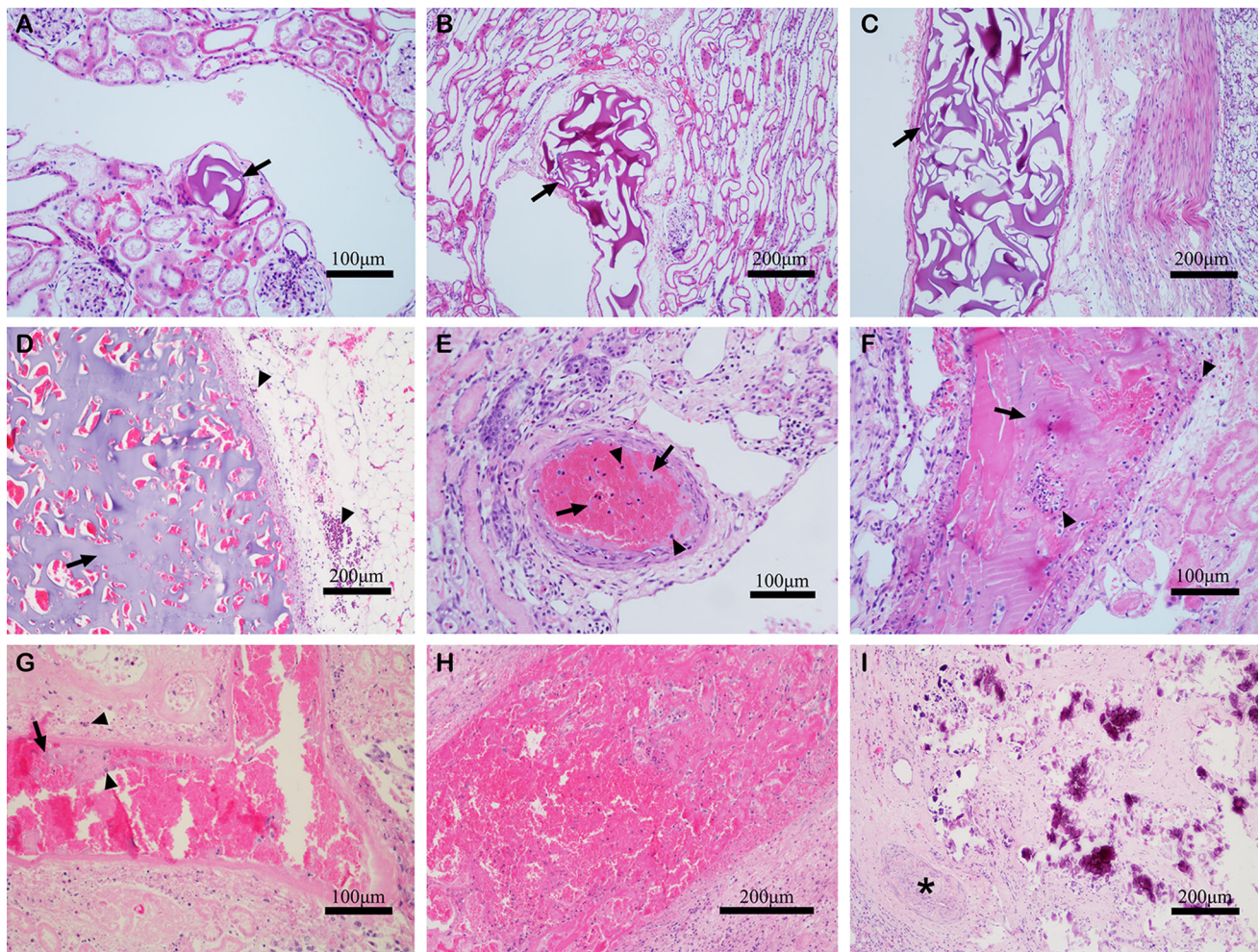


Fig. 6 Renal pathology after CGS particles embolization (hematoxylin–eosin-stained). **A–C** Immediately after embolization, CGS particles were found in interlobular, arcuate and interlobar arteries with a dense packing (arrow). No inflammation was observed. **D** Day 1, CGS particles were still observed with more compact distribution (arrow). Mild inflammation was observed (arrowheads). **E, F** Day 3, the degradation of the particles was first identified. A few gelation sponge particles were found in arcuate, while many in interlobar (arrow), along with partial vascular recanalization. Mild inflammation

was observed, which was more severe than day 1 (arrowheads). **G** Day 7, a few gelation sponge particles were found in interlobar (arrow), along with marked vascular recanalization. Mild inflammation was observed, which was less severe than day 3 (arrowheads). **H** Day 14, no gelatin sponge particles were found in interlobar. **I** Day 28, marked intimal hyperplasia was identified, which results in reocclusion of the recanalization vessels (star). The embolized renal parenchyma showed severe fibrosis and mineralization

range of the particles afforded by using a calibrated embolic agent helped to achieve better control and predictability of the level of target vessel occlusion [16]. Another advantage of CGS particles over handmade particles is the availability of smaller particles sizes such as 150–350 μm and 350–560 μm in diameter, whereas hand-cutting methods can only produce big particles in the range of 1000–1500 μm [15]. Smaller particles are more easily delivered via microcatheter during the superselective embolization procedures and reach more distal branch arteries while avoiding impaction of proximal branches. Because of this, the use of small particles in clinical practices is increasing [4, 12], and we choose 150–350 μm GS particles for this study.

After embolization, CGS particles were observed in the target lumen with dense packing. This may be attributed to the irregular shape and relatively uniform distribution of the particles. In addition, water absorption and compressibility properties of GS resulted in more compact embolization, as we observed in day 1. In our study, CGS particles were trapped in the interlobular artery. Oh et al. [17] found that hand-cut particles with an average diameter of 1 mm typically become trapped in the proximal artery (interlobar). This discrepancy indicates that calibrated GS particles of 150–350 μm can reach far more distal branches than hand-cut particles.

In this study, the degradation time of CGS particles is faster than that of the particles made by cutting. Meada

et al. [18] reported that 80% of GS particles made by manual cutting (about 1 mm in diameter) degraded before day 7 in the swine segmental embolized renal model, and vessel recanalization occurred. Another study by Louail et al. [19] showed that 63% of hand-cut GS particles (about 2–3 mm in diameter) started degradation on day 7 and degraded entirely by day 14, which was associated with a complete vascular recanalization. Furthermore, the complete degradation of CGS particles was first observed in interlobular branches, then in arcuate, and finally in interlobar arteries. These findings corroborate the claim that the smaller the particles are, the more quickly they degrade [19]. Compared to other bioresorbable embolic materials such as starch microspheres (with a resorption time of half an hour) and water-soluble polyvinyl alcohol microspheres (with a resorption time of 3 h), CGS particles have longer degradation periods [20, 21].

In this study, the vascular inflammation peaked at day 3 then diminished with the degradation of the GS particles. Only mild vascular inflammation without vascular necrosis was found. These findings suggest that GS particles have good biocompatibility, which is consistent with the study of porcine sponge reported by Louail et al. [19]. However, some scholars reported moderate inflammatory reactions and vascular necrosis when hand-cut GS particles of 1 mm were used [17]. This is likely due to the tendency for bigger particles to become trapped at higher embolic levels, which may lead to prolonged absorption of particles and consequently more severe inflammatory reactions. As Kawai et al. [3] demonstrated, faster absorption due to lower embolic level will reduce the degree of inflammation and vessel injury. Owing to their resorbability, the inflammation associated with CGS particles is self-limiting. That is, progressive degradation and eventual complete removal of the foreign material, in conjunction with restoration of blood flow, will ameliorate any inflammation. In contrast, nonresorbable particles are permanent, and the foreign body reaction will last for life [22].

CTA and histopathology analysis revealed that the recanalization of the target embolic arteries is associated with the degradation of CGS particles in the early observation phase. However, attenuation of embolized vessels was observed on day 28 and day 56. Ohta et al. [23] reported a similar finding that the perfusion rate decreased in the later phase after embolization by gelatin microspheres. Oh and colleagues reported significant stenoses in the recanalized arteries embolized by GS, mainly caused by organized thrombi and intimal hyperplasia [17]. In our study, no organized thrombi can be observed. The reason may be that the rate of thrombolysis exceeds the rate of organization, as the mild inflammation is associated with CGS particles. As the rate of thrombus organization is related in part to the magnitude of the inflammation

induced by the embolic agent, the more severe the inflammation, the more rapid the thrombus organization [24]. Intimal hyperplasia has been regarded as a significant pathophysiological cause of the high restenosis rate in the interventional environment [25]. This vascular pathology results in a progressive diminution of the vessel lumen [26]. Because intimal hyperplasia occurred 2 weeks after embolization [2], there were no observations of intimal hyperplasia in the early observation phases of our study. In the later phases; however, marked intimal hyperplasia resulting in the vessel lumen narrowed was observed. This may imply arterial wall damage because intimal hyperplasia is a nonspecific indicator for vessel injury. The arterial wall injury induced intimal hyperplasia [17], which was finally resulting in permanent vascular occlusion. The arterial wall injury may be caused by the mild inflammation associated with the CGS particles, as well as the reperfusion after the vessel recanalization [26]. Some scholars also reported that a dense packing of GS may be attributed to permanent vascular occlusion [9, 27], which is parallel with our observation. In addition, it is well known that renal parenchyma is very sensitive to ischemia. If ischemia lasts for more than four hours, irreversible damage to the renal glomerular and renal tubular will occur [28]. The embolized renal parenchyma did not heal after reperfusion of the blood flow. The vessel lumen inside the infarction narrowed progressively, which led to the diminishment of the vascular bed [23]. Then, autonephrectomy emerged, and evident fibrosis and mineralization could be observed in infarctions of the kidney.

Compared with hand-cut GS particles, CGS particles are smaller in size and have a more uniform distribution. Therefore, CGS particles have the advantages of more distal embolization, more accurate level of embolization and degradation period, and minimal inflammation compared to hand-cut GS particles. CGS particles are thus more effective embolic agents than hand-cut GS particles.

This study has some limitations. First, the renal artery is an end-artery with no collateral circulation. The occlusion of the renal artery induces renal infarction and this might influence the embolic characteristics of the GS particles. Ideally, to evaluate embolic effect, the hepatic or internal iliac artery should be considered because they are categorized as non-end arteries. However, it is technically difficult to perform an angiogram and embolization for the abovementioned arteries on the rabbit model. A larger animal model would be required for the execution of this experiment. Second, four blocks with pathological changes were selected per kidney, but just two sections per block were examined histologically. In some cases, the area of impaction of the particles may have been excluded from the section. Third, the results were obtained on a small sample size. The present findings have to be confirmed

experimentally on larger cohorts of animals. Fourth, GS particles studied were assessed at a size range of 150–350 μm , and the results may not be reasonably extrapolated to other size ranges.

In conclusion, CGS particles of 150–350 μm produced dense and distal embolization, and were resorbed before day 14 with a mild tissue reaction. Vessel recanalization occurred secondary to the resorption of gelatin sponge particles, but permanent vascular occlusion developed due to marked intimal hyperplasia after day 28.

Acknowledgements The authors are grateful to Wenlin Fan, from department of Radiology at Drexel University College of Medicine, Hahnemann University Hospital, Philadelphia, Pennsylvania, for the assistance in preparing the final version of our manuscript.

Compliance with Ethical Standards

Conflict of interest The authors declare that they have no conflict of interest.

Ethical Approval All applicable international, national, and/or institutional guidelines for the care and use of animals were followed. All procedures performed in studies involving animals were in accordance with the ethical standards of the institution or practice at which the studies were conducted.

References

- Loffroy R, Guiu B, Cercueil JP, Krause D. Endovascular therapeutic embolisation: an overview of occluding agents and their effects on embolised tissues. *Curr Vasc Pharmacol*. 2009;7(2):250–63.
- Miyayama S, Yamakado K, Anai H, Abo D, Minami T, Takaki H, et al. Guidelines on the use of gelatin sponge particles in embolotherapy. *Jpn J Radiol*. 2014;32(4):242–50.
- Kawai N, Sato M, Minamiguchi H, Ikoma A, Sanda H, Nakata K, et al. Clinical evaluation of transcatheter arterial chemoembolization with 2-day-soluble gelatin sponge particles for hepatocellular carcinoma-comparison with insoluble gelatin sponge particles. *J Vasc Interv Radiol*. 2013;24(9):1383–90.
- Kamran AU, Liu Y, Li FE, Liu S, Wu JL, Zhang YW. Transcatheter Arterial chemoembolization with gelatin sponge microparticles treated for BCLC stage B hepatocellular carcinoma: a single center retrospective study. *Medicine (Baltimore)*. 2015;94(52):e2154.
- Song YG, Jang H, Park KD, Kim MD, Kim CW. Non spherical polyvinyl alcohol versus gelatin sponge particles for uterine artery embolization for symptomatic fibroids. *Minim Invasive Ther Allied Technol*. 2013;22(6):364–71.
- Izumi Y, Ikeda S, Kitagawa A, Katsuda E, Hagihara M, Kamei S, et al. Uterine artery embolization by use of porous gelatin particles for symptomatic uterine leiomyomas: comparison with hand-cut gelatin sponge particles. *Jpn J Radiol*. 2015;33(8):461–70.
- Borsa JJ, Fontaine AB, Eskridge JM, Song JK, Hoffer EK, Aoki AA. Transcatheter arterial embolization for intractable epistaxis secondary to gunshot wounds. *J Vasc Interv Radiol JVIR*. 1999;10(3):297–302.
- Nijhof HW, Willemssen FE, Jukema GN. Transcatheter arterial embolization in a hemodynamically unstable patient with grade IV blunt liver injury: is nonsurgical management an option? *Emerg Radiol*. 2006;12(3):111–5.
- Jander HP, Russinovich NA. Transcatheter gelfoam embolization in abdominal, retroperitoneal, and pelvic hemorrhage. *Radiology*. 1980;136(2):337–44.
- Brown DB, Pilgram TK, Darcy MD, Fundakowski CE, Lisker-Melman M, Chapman WC, et al. Hepatic arterial chemoembolization for hepatocellular carcinoma: comparison of survival rates with different embolic agents. *J Vasc Interv Radiol JVIR*. 2005;16(12):1661–6.
- Katsumori T, Kasahara T. The size of gelatin sponge particles: differences with preparation method. *Cardiovasc Interv Radiol*. 2006;29(6):1077–83.
- Song YG, Woo YJ, Kim CW. Uterine artery embolization using progressively larger calibrated gelatin sponge particles. *Minim Invasive Ther Allied Technol*. 2016;25(1):35–42.
- Weng L, Seelig D, Rostamzadeh P, Golzarian J. Calibrated bioresorbable microspheres as an embolic agent: an experimental study in a rabbit renal model. *J Vasc Interv Radiol JVIR*. 2015;26(12):1887–94.e1.
- Ohta S, Nitta N, Takahashi M, Murata K, Tabata Y. Degradable gelatin microspheres as an embolic agent: an experimental study in a rabbit renal model. *Korean J Radiol*. 2007;8(5):418–28.
- Abada HT, Golzarian J. Gelatine sponge particles: handling characteristics for endovascular use. *Tech Vasc Interv Radiol*. 2007;10(4):257–60.
- Pelage JP, Laurent A, Wassef M, Bonneau M, Germain D, Rymer R, et al. Uterine artery embolization in sheep: comparison of acute effects with polyvinyl alcohol particles and calibrated microspheres. *Radiology*. 2002;224(2):436–45.
- Oh JS, Lee HG, Chun HJ, Choi BG, Choi YJ. Evaluation of arterial impairment after experimental gelatin sponge embolization in a rabbit renal model. *Korean J Radiol*. 2015;16(1):133–8.
- Maeda N, Verret V, Moine L, Bédouet L, Louguet S, Servais E, et al. Targeting and recanalization after embolization with calibrated resorbable microspheres versus hand-cut gelatin sponge particles in a porcine kidney model. *J Vasc Interv Radiol JVIR*. 2013;24(9):1391–8.
- Louail B, Sapoval M, Bonneau M, Wasseff M, Senechal Q, Gaux JC. A new porcine sponge material for temporary embolization: an experimental short-term pilot study in swine. *Cardiovasc Interv Radiol*. 2006;29(5):826–31.
- Shomura Y, Tanigawa N, Shibutani M, Wakimoto S, Tsuji K, Tokuda T, et al. Water-soluble polyvinyl alcohol microspheres for temporary embolization: development and in vivo characteristics in a pig kidney model. *J Vasc Interv Radiol JVIR*. 2011;22(2):212–9.
- Pieper CC, Meyer C, Vollmar B, Hauenstein K, Schild HH, Wilhelm KE. Temporary arterial embolization of liver parenchyma with degradable starch microspheres (EmboCept®S) in a swine model. *Cardiovasc Interv Radiol*. 2015;38(2):435–41.
- Stampfl U, Stampfl S, Bellemann N, Sommer CM, Lopez-Benitez R, Thierjung H, et al. Experimental liver embolization with four different spherical embolic materials: impact on inflammatory tissue and foreign body reaction. *Cardiovasc Interv Radiol*. 2009;32(2):303–12.
- Ohta S, Nitta N, Watanabe S, Tomozawa Y, Sonoda A, Otani H, et al. Gelatin microspheres: correlation between embolic effect/degradability and cross-linkage/particle size. *Cardiovasc Interv Radiol*. 2013;36(4):1105–11.
- Sniderman KW, Sos TA, Alonso DR. Transcatheter embolization with Gelfoam and Avitene: the effect of Sotradecol on the duration of arterial occlusion. *Investig Radiol*. 1981;16(6):501–7.

25. Liu MW, Roubin GS, King SB. Restenosis after coronary angioplasty. Potential biologic determinants and role of intimal hyperplasia. *Circulation*. 1989;79(6):1374–87.
26. Mills B, Robb T, Larson DF. Intimal hyperplasia: slow but deadly. *Perfusion*. 2012;27(6):520–8.
27. Barth KH, Strandberg JD, White RI. Long term follow-up of transcatheter embolization with autologous clot, oxycel and gel-foam in domestic swine. *Investig Radiol*. 1977;12(3):273–80.
28. Leary FJ, Utz DC, Wakim KG. Effects of continuous and intermittent renal ischemia on renal function. *Surg Gynecol Obstet*. 1963;116:311–7.

Publisher's Note Springer Nature remains neutral with regard to jurisdictional claims in published maps and institutional affiliations.